

February 9, 2018 18:18

ON THE ORIGIN OF VERY HIGH ENERGY COSMIC RAYS

PASQUALE BLASI

INAF/Osservatorio Astrofisico di Arcetri

Largo E. Fermi, 5 - I50125 Firenze (ITALY)

Received Day Month Year

Revised Day Month Year

We discuss the most recent developments in our understanding of the acceleration and propagation of cosmic rays up to the highest energies. In particular we specialize our discussion to three issues: 1) developments in the theory of particle acceleration at shock waves; 2) the transition from galactic to extragalactic cosmic rays; 3) implications of up-to-date observations for the origin of ultra high energy cosmic rays (UHECRs).

1. Introduction

The spectrum of cosmic rays observed at the Earth between 10^{11} eV and 10^{21} eV is illustrated in Fig. 1: at energies below 100 GeV the observed spectrum is heavily affected by local phenomena such as the interaction with the solar wind and the magnetic field of the Earth. In Fig. 1, the flux has been multiplied by E^3 in order to emphasize the possible departures from a power law E^{-3} . There are basically three features that may be identified in such spectrum: 1) a knee at energy $E_K \approx 3 \times 10^{15}$ eV, consisting of a steepening of the all-particle spectrum from $E^{-2.7}$ to $\sim E^{-3}$; 2) a second knee at energy $E_{2K} \approx 10^{18}$ eV; 3) a dip at $E_D \approx 5 \times 10^{18}$ eV. While all of these features result from observations, a fourth feature has been predicted to exist on pure theoretical grounds, though it has not been observed yet, mainly because of the insufficient statistics of collected events: at energies $\geq 10^{20}$ eV, the photopion production interactions of protons with the cosmic microwave background should produce a suppression in the flux, the so-called *Greisen-Zatsepin-Kuzmin (GZK) feature*¹. The detection of such feature would represent the best proof that these cosmic rays are of extragalactic origin.

While the detection of the GZK feature has been and in fact is one of the most important goals for cosmic ray physics, for the implications that it has on both physics and astrophysics, the problem of the origin of cosmic rays as a whole includes many more issues and open problems. It appears clear from recent findings that the collection of high statistics of events and credible measurements of the chemical composition are crucial ingredients for the understanding of the phenomenon at all energies. At energies above $\sim 10^{17}$ eV, the measurements of anisotropy also become a very precious tool.

In this review we limit our discussion to three issues that appear particularly

important at the present time: 1) the acceleration of cosmic rays through diffusive motion across shock fronts (Sec. 2); 2) the transition from cosmic rays accelerated within our Galaxy to those that reach us from extragalactic sources (Sec. 3); 3) the spectrum and small scale anisotropies of UHECRs (Sec. 4). We summarize in Sec. 5.

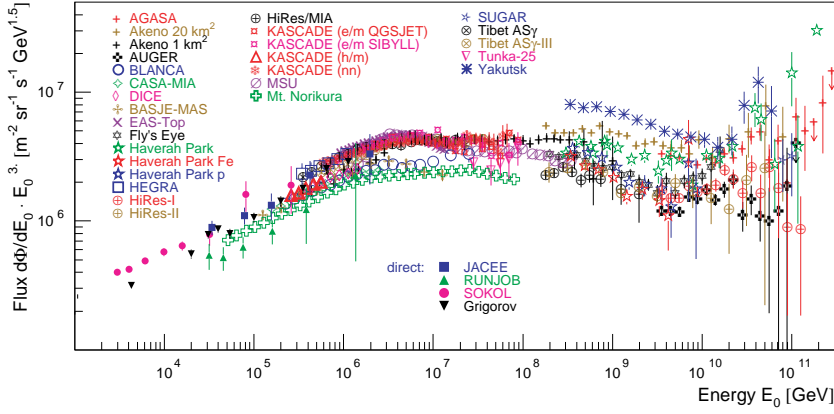


Fig. 1. All-particle spectrum of cosmic rays as observed at the Earth (collection of data from several experiments as in Ref. ²⁰. The references to the experiments listed in the figure can also be found in Ref. ²⁰.)

2. Diffusive acceleration of cosmic rays at collisionless shocks

2.1. Non-relativistic shocks: a paradigm confronting observations

The paradigm that is generally invoked to explain the origin of the bulk of galactic cosmic rays is based on the acceleration of particles at collisionless non-relativistic shock waves that develop in the supersonic motion of the ejecta of supernova explosions ² (see ³ for a recent excellent review and ⁴ for a broader view of the subject). Particle acceleration at similar shocks in other sources (e.g. active galaxies, radio lobes) is often invoked to explain the origin of higher energy cosmic rays.

Building on the original idea of Fermi ⁵, in the 70's a deep investigation of stochastic acceleration in the presence of shock waves was started ^{6,7,8} (see ^{10,9,31} for reviews). The scattering of charged particles back and forth through the shock front was shown to lead to energization of the particles. The advection of the accelerating particles with the fluid towards downstream infinity is responsible for the formation of a spectrum which has the form of a power law in momentum. In the case of strong shock waves (Mach number $M \gg 1$) the spectrum tends asymptotically to have a spectrum $\propto E^{-\gamma}$ with slope $\gamma \sim 2$ ^{6,7 a}.

^aHere and in the following we will use the expression *slope γ of the spectrum* when we refer

For cosmic rays that are originated in the Galaxy and reach the Earth through a diffusive wandering motion, the spectra get modified by diffusion, so that an injection spectrum $Q(E) \propto E^{-\gamma}$ is steepened to an equilibrium spectrum $n(E) \approx Q(E)\tau_{dif}(E) \propto E^{-(\gamma+\alpha)}$, where $\tau_{dif}(E) \propto 1/D(E)$ is the diffusion time for particles with energy E and $D(E) \propto E^\alpha$ is the diffusion coefficient. Energy losses and turbulent reacceleration (namely second order Fermi acceleration) can slightly but not substantially affect this result at energies larger than ~ 100 GeV¹¹. Fragmentation of heavy nuclei changes the slope of the observed spectra for those chemical elements for which these processes are relevant (most notably iron). The diffusion coefficient in the interstellar medium (ISM) can be inferred from the abundances of light elements (primarily Lithium, Boron and Berillium, scarce in the primordial soup and not appreciably synthesized in stars), produced almost entirely through spallation of heavier elements (see ref. ¹² and references therein). From the measurement of the abundance of these light elements (as well as from other observational constraints, widely discussed in ¹³ and references therein) it is possible to infer an estimate of the typical time of residence of cosmic rays with energy ~ 1 GeV in the Galaxy. This time turns out to be of several million years, the best proof that cosmic rays diffuse in the Galaxy (the crossing time for straight line propagation would be only $\leq 3 \times 10^4$ years).

For our purposes we can adopt as an order of magnitude for the diffusion coefficient in the Galaxy $D_{gal}(E) \approx 3 \times 10^{29} (E/GeV)^\alpha$ cm²s⁻¹, with $\alpha \approx 0.6$ ($\alpha = 1/3$ would correspond to Kolmogorov spectrum of fluctuations and would imply a somewhat smaller normalization. $\alpha = 0.5$ corresponds to Kraichnan diffusion). The observed spectrum at energies below the knee forces $\gamma + \alpha = 2.7$ while leaving the two slopes separately unconstrained. If indeed $\alpha = 0.6$, the injection spectrum would be forced to be $\propto E^{-2.1}$ ^b

The maximum energy of the accelerated particles is the main concern for the scenario just outlined: if the supernova explosion occurs in the ISM, the diffusion coefficient that determines the motion of the particles upstream of the supernova shock is of the order of $D_{gal}(E)$ (see above). The acceleration time is therefore $\tau_{acc}(E) \approx D_{gal}(E)/u_{sh}^2$, where u_{sh} is the shock velocity (\sim a few 1000 km/s). For a supernova remnant of typical age $\tau_{SNR} \sim 1000$ years, the maximum energy of protons is easily estimated by requiring that the acceleration time remains smaller than τ_{SNR} , and it is found to be of the order of *fractions of GeV*. The maximum energy of electrons is determined by the balance between acceleration and energy losses.

This estimate strongly suggests that acceleration of protons is possible only if the

to the distribution function in energy space, so that the total number of particles is given by $\int dE f(E)$. We will use the symbol γ_p or s to refer to the slope of the distribution function of accelerated particles in momentum space, normalized in such a way that the number of particles is $\int dp 4\pi p^2 f(p)$. Clearly $\gamma_p = 2 + \gamma$ for ultra relativistic particles.

^bIt is not clear if this slope of the diffusion coefficient is compatible with the observed anisotropy above the knee (see ³ for details and additional references).

diffusion coefficient close to the shock is much smaller than that in the interstellar medium. One realistic way to achieve this condition is to allow for the self-generation of magnetic turbulence by the accelerated particles⁸: if charged particles move in a magnetized medium with a bulk velocity that exceeds the Alfvèn speed, the *streaming instability* is excited, thereby limiting the speed of the bulk of cosmic rays to roughly the Alfvèn speed. In this case the diffusion coefficient upstream of the shock is determined by the density of accelerated particles. In the context of quasi-linear theory the form of the diffusion coefficient can be written as $D(E) = D_B(E)/\mathcal{I}$, where $D_B(E) = (1/3)r_L(E)c$ is the Bohm diffusion coefficient (r_L here is the Larmor radius of particles with energy E). \mathcal{I} is the energy density of Alfvén waves resonant with particles with energy E relative to the background magnetic field B :

$$\frac{\delta B^2}{8\pi} = \frac{B^2}{8\pi} \int \frac{dk}{k} \mathcal{I}(k). \quad (1)$$

In terms of quasi-linear theory, the value of \mathcal{I} is bound to be less than unity. If $\mathcal{I} = 1$ (strong turbulence), then diffusion occurs in the the Bohm regime^{8,14}. In^{14,15} the authors demonstrate that the maximum energy of protons within this scenario is as large as $E_{max} \approx 10^{13} - 10^{14}$ eV, and Z times larger for heavier nuclei with charge Z . Despite this improvement, the E_{max} obtained in¹⁴ is still ~ 30 times smaller than the energy at which the knee is measured (see Fig. 1).

This relatively low value of E_{max} is the direct consequence of assuming that the saturation of the self-generated turbulence occurs when the linear theory breaks down, namely when $\mathcal{I} \sim 1$. This might be the case if the fraction of energy channelled into cosmic rays is small, $P_{CR} \ll \rho u^2$. On the other hand, the maximum theoretical saturation level that can be predicted, even in the context of quasi-linear theory, is much higher, as was found in¹⁶, by simply using the basic equation that describes the amplification and convection of waves:

$$u \frac{d\mathcal{F}(k)}{dx} = v_A \frac{d\mathcal{P}_{CR}}{dx}, \quad (2)$$

where u is the shock speed, v_A is the Alfvèn speed (calculated using the background unperturbed magnetic field) and $\mathcal{F} = \frac{B^2}{8\pi}\mathcal{I}$ is the energy density in the waves with wavenumber k ^c. The pressure \mathcal{P}_{CR} in Eq. 2 is the one that refers to particles with momenta p that can resonate with waves with wavenumber k , namely those for which $k^{-1} = p|\mu|/ZeB$, where the wavenumber k is assumed to be parallel to the direction of the background magnetic field and μ is the pitch angle of the particle.

^cThe correct equation should in fact be

$$\frac{\partial \mathcal{F}}{\partial t} + (u + v_A) \frac{\partial \mathcal{F}}{\partial x} = v_A \frac{d\mathcal{P}_{CR}}{dx}.$$

Here we are assuming that a stationary situation is reached and that the fluid is strongly super-alfvenic, $u \gg v_A$.

If one assumes a sharp resonance at $p = p_{res} = ZeB/ck$, then

$$\mathcal{P}_{CR} = \frac{4\pi}{3} p_{res}^4 v(p_{res}) f(p_{res}).$$

If one is interested in the total magnetic field amplification δB^2 , as defined in Eq. 1, then the previous equation becomes

$$u \frac{d}{dx} \frac{\delta B^2}{8\pi} = v_A \frac{dP_{CR}}{dx}, \quad (3)$$

where now P_{CR} is the total cosmic rays pressure at the shock.

Integration of this equation implies that

$$\frac{\delta B^2}{B^2} = 2M_A \frac{P_{CR}}{\rho u^2}, \quad (4)$$

where M_A is the Alfvén Mach number. If $P_{CR} \sim \rho u^2$, the amplification of the magnetic field with respect to the background undisturbed field can be as high as $M_A^{1/2}$. Several processes can reduce the effective magnetic field to values much lower than those found through Eq. 4¹⁷. On the other hand, 4 immediately shows that the linear theory that it is based upon is easily broken in the description of efficient particle acceleration at shocks.

Some authors have argued that shock acceleration in the denser environment of some pre-supernova environments could help reaching energies higher than or comparable with those predicted by ^{18,19}. This scenario may take place in some sources and may work together with the process of self-amplification of the magnetic field explained above.

The concern about the highest energy of particles accelerated at SNRs has become even more serious with the recent findings of the KASCADE experiment that could measure the spectra of different chemical elements separately. A collection of the data for protons and helium nuclei from several experiments is shown in Fig. 2 (from Ref. ²⁰). For heavier elements the uncertainties in the data become large and prevent to reach useful conclusions at the present time. For our purposes the con-

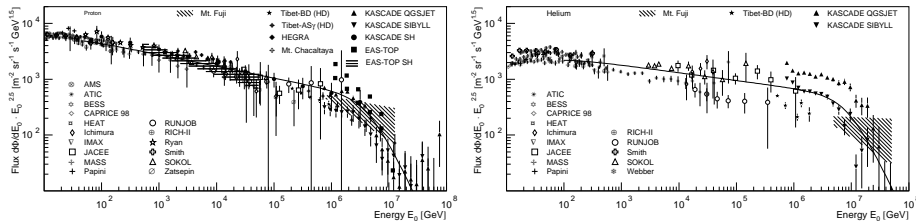


Fig. 2. Spectrum of protons (left panel) and helium nuclei (right panel) as reported in Ref. ²⁰.

tinuous lines ²¹ can be used just to guide the eye. The KASCADE data ²² suggest the intriguing possibility that the observed knee in the all-particle spectrum may

result from the superposition of different power laws, each describing the spectrum of different chemical components, and each with a rigidity dependent knee. If this interpretation is confirmed, then the *observed* knee in the all-particle spectrum may not have direct physical meaning and the knees in the single components would require an explanation, either in terms of acceleration in the sources or in terms of propagation in the Galaxy (see Ref. ²³ for an attempt at explaining these knees in terms of acceleration in SNRs).

Two pieces of information can be inferred from Fig. 2: 1) protons are measured up to energies $(2 - 4) \times 10^{16}$ eV, that exceeds the maximum energy predicted by standard diffusive shock acceleration by at least two orders of magnitude. Helium nuclei are measured up to energies roughly twice as large as those of protons, as would be expected on the basis of a rigidity dependent process; 2) Protons and Helium each seem to have their own rigidity dependent *knees*. The spectrum above these knees is characterized by a steepening rather than a cutoff (the approximate slopes are ~ 2.7 below the knees and ~ 3.8 above). Following the same rigidity criterion, iron nuclei would have their knee at $E_{Fe} \sim 4 \times 10^{16}$ eV and maximum energies at $\geq 10^{17}$ eV. Unfortunately no solid conclusion on heavy nuclei can be reached from the data at the present time.

We will discuss the possible implications of point 2) in Sec. 3. Here we wish to discuss the very basic issue of the maximum energy of particles accelerated at shock waves. Although the main conclusions will apply to shocks in SNRs, similar considerations might be reached, on the case by case basis, for sites of acceleration of UHECRs where shocks are invoked.

We have already pointed out that the linear theory of particle acceleration at shock waves fails to explain maximum energies as high as that of the knee by a factor ~ 30 and it fails to explain proton energies as high as those measured by KASCADE and shown in Fig. 2 by a factor ~ 100 . In the following we shall describe how recent developments of non-linear theories of particle acceleration may change this conclusion dramatically.

One of the main achievements of recent investigations on particle acceleration at collisionless shock waves consists of having introduced the reaction of the accelerated particles onto the accelerating shock and the fluid itself. These modern theories no longer treat the accelerated particles as test particles. This phenomenon has received much attention in the context of the so-called two-fluid models ^{24,25}, kinetic models ^{26,27,28,29,30,40} and numerical approaches, both Monte Carlo and other numerical procedures ^{31,32,33,34,35,36,37,38}. For a relatively recent accurate review see the work by ³⁹, which also contains a discussion of the role of injection of protons and electrons.

These independent approaches confirm that the cosmic ray reaction enhances the acceleration efficiency and at the same time flattens the spectra of particles at the highest energy end (close to the maximum energy). Typical spectra and slopes of the accelerated particles are shown in Fig. 3 (from Ref. ⁴⁰) as obtained with an exact solution applicable to arbitrary diffusion properties of the plasma: the

upper panel shows the spectra obtained for maximum energy of 10^5 GeV and Mach number of the shock as in the caption. The lower panel shows the local slope as a function of momentum ($q(p) = -d \log f(p) / d \ln p$). The predicted spectra, which are no longer power laws, are typically softer than the linear prediction at low energy and harder (as hard as $f(p) \propto p^{-3.2}$) at the highest energies.

The concave spectra obtained in the context of non-linear particle acceleration at shock fronts reflect the formation of a precursor in the upstream fluid, namely a region with a size of the order of the diffusion length of the highest energy particles, in which the density and velocity profiles are space dependent. More specifically, the fluid speed increases whereas density decreases while moving away from the shock itself. This results in the appearance of a compression factor that is a function of the distance from the shock: the total compression factor R_{tot} between upstream infinity and downstream can reach values much larger than the classical strong shock limit, $R_{tot} \gg 4$, while for the compression factor at the gaseous shock $R_{sub} \leq 4$. Particles with different momenta *feel* different compressions and this is reflected into the appearance of non-power-law spectra, as shown in Fig. 3. The shock modification that we just explained is somewhat reduced due to the transfer of energy from cosmic rays to the thermal gas, as a consequence of Alfvèn heating^{41,16} or Drury instability⁴².

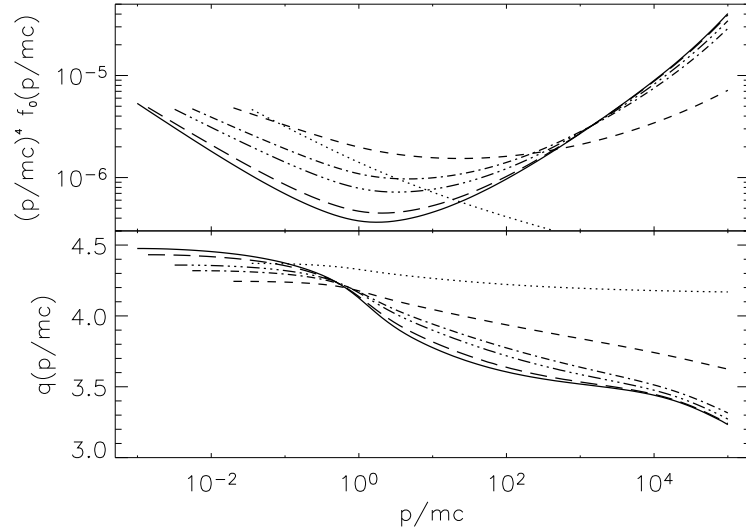


Fig. 3. *Upper panel:* Spectra of accelerated particles at the location of the shock for $M_0 = 4$ (dotted line), 10 (short-dashed line), 50 (dash-dotted line), 100 (dash-dot-dot-dotted line), 300 (long-dashed line) and 500 (solid line). *Lower panel:* momentum dependent slope for the same values of Mach numbers.

It is important to realize however that these spectra are *instantaneous spectra*

and need to be convolved with the time evolution of the supernova parameters in order to provide the spectrum of cosmic rays originated from the supernova remnant of interest. The particles that are detected at the Earth as cosmic rays are liberated from the downstream region of the SNR only after the supernova shock dies out^d. Current calculations (not including the magnetic field amplification induced by cosmic rays) predict curved spectra as a result of this temporal evolution (see for instance 43). It is not clear if this curvature may be compatible with the steep power law spectra observed at the Earth, as it is not known how the magnetic field amplification at the shock location during the supernova evolution may change this result.

A specific prediction of these nonlinear approaches is that it is typical to have situations in which the pressure of cosmic rays becomes comparable with the total available kinetic energy of the fluid, $P_{CR} \sim \rho u^2$ and most of this pressure is actually carried by the particles with the highest momenta, another important difference with the case of acceleration in the linear regime.

The fact that P_{CR} and ρu^2 may be comparable changes considerably the development of the streaming instability with respect to the original calculations in 8,14. This has recently been investigated by 44,45,46 who in fact claim that the background magnetic field close to the shock may be amplified by a factor up to $\sim 10^3$. The most straightforward implication is that the corresponding maximum energy of the accelerated particles is larger than found by 14 by the same factor. It follows that the maximum energy predicted for protons would be $E_{max}^p \approx 10^{16} - 10^{17}$ eV, while being Z times larger for nuclei with charge Z . While there may be some effects that may saturate the instability to lower values of the turbulent magnetic field, this remains certainly an exciting development that has the potential to change our picture of particle acceleration in SNRs and in other scenarios as well, and in particular in the potential sources of ultra high energy cosmic rays. Another possible avenue to enhance the maximum energy of accelerated particles at cosmic ray modified shocks has been recently proposed in 47.

The main result, discussed in detail in 46 is that the efficient particle acceleration is responsible for a new branch of purely growing non-alfvenic modes, in the quasi-linear regime. The growth of these waves is found to be faster than that of Alfvénic modes and may be responsible for saturation at a level which is appreciably higher than that found in Eq. 4. In particular the saturation found by 46 with the help of numerical simulations is $\frac{\delta B^2}{8\pi} \approx \frac{u}{2c} P_{CR}$, namely

$$\frac{\delta B^2}{B^2} = M_A^2 \frac{u}{c} \frac{P_{CR}}{\rho u^2}. \quad (5)$$

By comparing this with Eq.4, we can see that the really new result is the different saturation level of the self-induced turbulence: for efficient particle acceleration, Eq.

^dIn principle only particles with momenta close to p_{max} can escape from the upstream region. In the context of non-linear particle acceleration at shocks however, these particles carry a non negligible fraction of the total cosmic ray energy density

4 provides $\delta B/B \sim M_A^{1/2}$, while Eq. 5 gives the much higher $\delta B/B \sim M_A(u/c)$. One should notice that Eq. 2 cannot be applied in a straightforward way to the unstable modes found in 46, because the term on the right hand side of that equation only applies to the growth rate of Alfvèn waves.

It is worth stressing that the calculations of 44,45,46 are actually not currently carried out in a self-consistent way: they all *assume* that $P_{CR} \sim \rho u^2$ but the calculations of the cosmic ray induced instabilities are performed assuming power law spectra of accelerated particles and spatially independent profiles of the background quantities (velocity, density, magnetic field) in the cosmic ray precursor (both these assumptions are known to be not fulfilled, but at present it is not clear what the consequences of relaxing these assumptions might be).

The results illustrated above are based on two related but separate arguments:
1) the particle acceleration at non-relativistic shocks occurs with a large efficiency;
2) this efficient acceleration is able to amplify the magnetic field.

It is easily understandable that this implies a quite non-linear scenario in which the spectrum of cosmic rays determines the spectrum of magnetic fluctuations, which in turn determines the diffusive properties felt by cosmic rays and therefore their spectrum. The amplification of the magnetic field also implies that the maximum energy of the accelerated particles increases, which in turn enhances the shock modification.

Despite all these promising developments on the theoretical side, the direct evidence of acceleration of hadrons at the shocks developed in SNRs is still missing. The smoking gun could come from the detection of gamma rays generated in the decay of neutral pions coming from inelastic nucleus-nucleus collisions. The recent detection of gamma rays by HESS 48 might be the long searched signal, but this needs further confirmation. However, indirect circumstantial evidences of efficient acceleration of hadrons and of magnetic field enhancement are not lacking. The concave spectra that are the peculiar feature of acceleration at strongly modified shocks might be required to explain the multifrequency observations of some SNRs 49. Although the radiations are produced by electrons, the latter are actually accelerated in the velocity background generated by the dynamical backreaction of protons, since electrons hardly contribute any pressure when compared with the hadronic component.

The recent paper by 50 provides us with a review of the magnetic fields inferred in several SNRs as obtained from the X-ray brightness of the shells. X-rays are generated by synchrotron emission of relativistic electrons, and the extension of the X-ray bright region depends on the strength of the magnetic field. The stronger the field the narrower the emitting region. In all cases considered by 50 the inferred fields are in the range of a few $100\mu G$, suggesting a substantial magnetic field amplification, possibly induced by cosmic rays. The authors of Ref. 51 have however argued that on the same spatial scale of the variations in the X-ray brightness a substantial damping of the amplified magnetic field is also expected. In this case

the observed variations in the X-ray brightness would reflect the damping of the magnetic field rather than the energy losses of energetic particles.

2.2. Relativistic shocks

For non-relativistic shocks the high velocity of the accelerated particles (\sim the speed of light) compared with the shock speed makes the particle distribution quasi-isotropic. This is no longer true for relativistic shocks, where the shock and the particles share roughly the same speed and there is not enough time for isotropizing the particles. This fact makes the acceleration qualitatively and quantitatively different in the case of relativistic shocks. An initially isotropic distribution of particles in the upstream fluid is transformed by the shock into a highly anisotropic distribution due to relativistic beaming, provided the particles can make their way back from the downstream region.

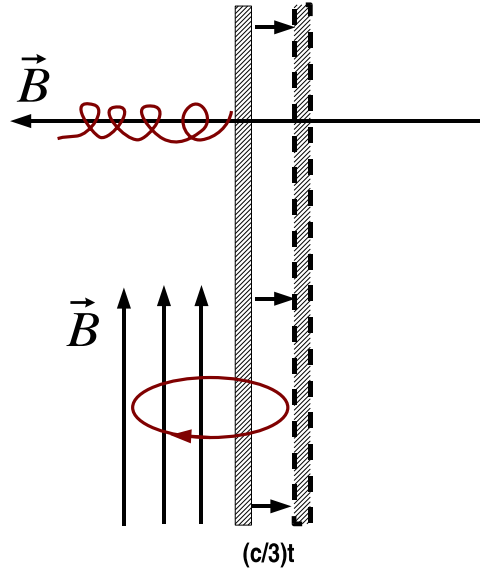


Fig. 4. Schematic view of particle acceleration at a relativistic shock without magnetic scattering agents. The case depicted at the top (bottom) refers to a magnetic field parallel (perpendicular) to the shock normal.

In Fig. 4 we plot a schematic view of acceleration at a relativistic shock front in the absence of scattering agents in the downstream plasma. The top (bottom) part shows the case of a magnetic field parallel (perpendicular) to the shock normal (case I and case II respectively). In the downstream frame of an ultra-relativistic shock the shock itself moves with a velocity $\sim c/3$. During the time $t = 2\pi r_L/c$ necessary

for relativistic particles to travel one Larmor rotation, the shock has moved by

$$\Delta x \sim \frac{1}{3}c \frac{2\pi r_c}{c} = \frac{2\pi}{3} r_L > r_L. \quad (6)$$

This implies that in the absence of magnetic scattering, it is virtually impossible for particles to re-cross the shock and take part in the acceleration process. Many different approaches have shown however that scattering helps in taking the particles back upstream (see for instance the simulations in Refs. 52,54,53,57 and the analytical approaches by 56,53,55,58,59).

Contrary to what happens in the case of non-relativistic shocks, the spectrum of particles accelerated at relativistic shocks is not universal, though being a power law. The slope of the spectrum depends on the details of the scattering of the particles in the upstream and downstream regions. In particular, if the *small pitch angle scattering* (SPAS) assumption is made, then some kind of universality is recovered for large Lorentz factors $\gamma_{sh} \gg 1$, and the slope of the distribution function in momentum space approaches $s = 4.32$ 55,54,59. On the other hand at some sufficiently large value of γ_{sh} the assumption of SPAS is expected to break. At this point it is expected that the spectrum hardens 59 with respect to the *universal* spectrum.

The slope is also demonstrated to depend on the equation of state of the gas downstream, which determines the compression factor at the shock. For instance, for a shock speed $u = 0.9$ in units of the speed of light, the spectrum in momentum space has a slope $s = 4.71$ for the case of the so-called relativistic equation of state $u u_d = 1/3$ (u_d here is the speed of the downstream fluid in the shock frame), but it is $s \sim 4.1$ for the probably more realistic Synge equation of state 60. In the left panel of Fig. 5 (from 59) we plot the predicted spectral slope as a function of the shock compression factor for $u = 0.8$ and $u = 0.9$.

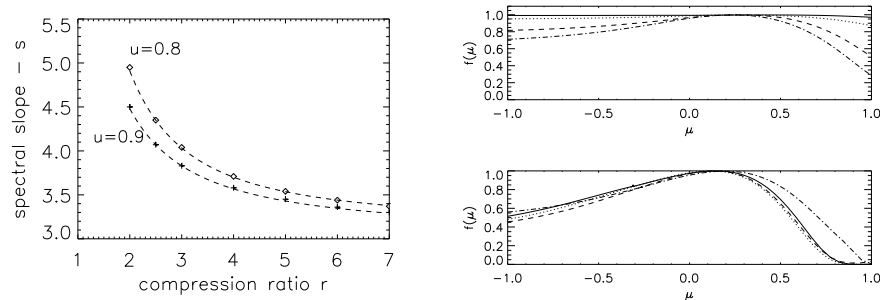


Fig. 5. [On the Left]- Slope of the spectrum of accelerated particles for a shock with speed $u = 0.8$ (diamonds - upper curve) and $u = 0.9$ (crosses - lower curve) in the regime of large angle scattering, as a function of the compression ratio. The continuous lines are the fit to the results of Ref. 61. [On the right]- Upper panel: Distribution function for $\gamma_{sh}\beta_{sh} = 0.04$ (solid line), $\gamma_{sh}\beta_{sh} = 0.2$ (dotted line), $\gamma_{sh}\beta_{sh} = 0.4$ (dashed line) and $\gamma_{sh}\beta_{sh} = 0.6$ (dash-dotted line). Lower panel: Distribution function for $\gamma_{sh}\beta_{sh} = 1$ (dash-dotted line), $\gamma_{sh}\beta_{sh} = 2$ (dashed line), $\gamma_{sh}\beta_{sh} = 4$ (dotted line) and $\gamma_{sh}\beta_{sh} = 5$ (solid line).

As qualitatively explained above, the distribution function of particles accelerated at shocks moving at speed close to the speed of light is expected to be anisotropic, both upstream and downstream. In the right panel of Fig. 5 (from ⁵⁹) we show the downstream distribution function for the shock speeds listed in the caption, as calculated in Ref. ⁵⁹. It is clear how the anisotropy increases when the shock becomes increasingly more relativistic. The slopes in momentum space for the cases considered in Fig. 5 (right panel) are listed in Table 1 ⁵⁹.

$\gamma_{sh}\beta_{sh}$	u	u_d	slope s
0.04	0.04	0.01	4.00
0.2	0.196	0.049	3.99
0.4	0.371	0.094	3.99
0.6	0.51	0.132	3.98
1.0	0.707	0.191	4.00
2.0	0.894	0.263	4.07
4.0	0.97	0.305	4.12
5.0	0.98	0.311	4.13

The phenomenon of shock modification induced by cosmic rays has received much less attention for the case of relativistic shocks (see ⁶² and ⁶³).

3. The transition from galactic to extragalactic origin: an ankle or a dip?

The structure formed by the second knee and the dip, illustrated in Fig. 1, has been traditionally interpreted as the transition from galactic to extragalactic cosmic rays, and named *the ankle*. This rather sharp feature would be the result of the superposition of a rapidly falling galactic spectrum and a rising (in the $E^3 J(E)$ formalism) spectrum of extragalactic cosmic rays. This scenario requires that the cutoff in the galactic component exceeds 10^{19} eV.

More recently an alternative interpretation has been put forward, with very significant implications for the origin of cosmic rays at large. In ^{64,65} it was pointed out that the combination of pair production energy losses and adiabatic energy losses, due to the expansion of the universe, would generate a spectrum of cosmic rays at the Earth with a feature which fits the observed second knee and dip (see Fig. 6 for predictions obtained following the calculations of ^{66,64,65}). We will refer to this model as the *twisted ankle* (TWA) scenario. In this model the transition from galactic to extragalactic cosmic rays would take place at energies below $\sim 10^{18}$ eV, where the galactic cosmic rays would be cut off. Much larger maximum energies of galactic cosmic rays are required in the *ankle* scenario, where the galactic component disappears only at $E \geq 10^{19}$ eV. In its basic form, the TWA scenario implies that cosmic rays are injected at extragalactic sources with an injection spectrum $E^{-2.7}$ and no luminosity evolution (solid line in Fig. 6). Although it is a worse fit, the data appear to show a dip-like structure also for the case of evolving sources, with

injection spectrum $E^{-2.4}$ and luminosity evolution that scales with the redshift z of the sources as $L(z) \propto (1+z)^4$ (dashed line in Fig. 6). In both cases, even small levels of magnetization of the intergalactic medium would induce a low energy suppression of the flux, which might in fact improve the fit to the all-particle spectrum 67,68.

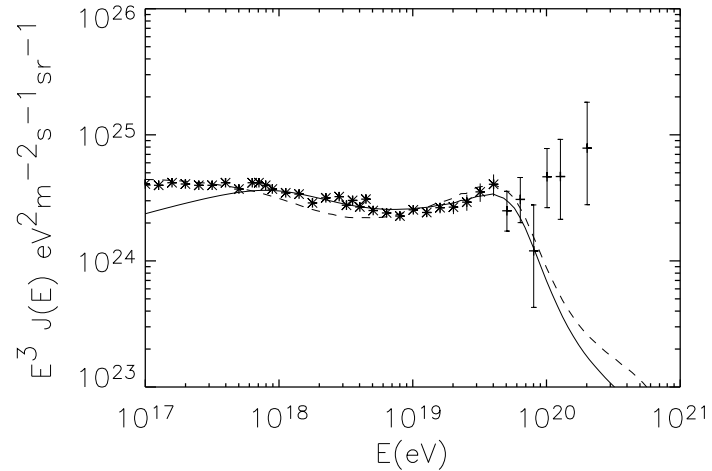


Fig. 6. Spectrum of cosmic rays of extragalactic origin for an injection spectrum $\propto E^{-2.7}$ and no luminosity evolution (solid line) and for injection spectrum $\propto E^{-2.4}$ and luminosity evolution $L(z) \propto (1+z)^4$ (dashed line). The data are from Akeno and AGASA.

The most appealing aspects of the TWA scenario can be summarized as follows: 1) the dip is a natural consequence of particle physics: it is simply produced by the combination of adiabatic energy losses and Bethe-Heitler losses. 2) the model does not require galactic sources to accelerate cosmic rays to energies in excess of 10^{19} eV, which would represent a problem for the vast majority of acceleration models applied to galactic sources (see however 69,70 for a model in which acceleration of nuclei to such energies is achieved, although with too flat a spectrum to be relevant for this physical situation).

If the rigidity model suggested by the KASCADE data and discussed in Sec. 2 is correct, it is not easy to argue in favor of a heavy nuclear component extending to energies $> 10^{19}$ eV. Although this point is rather weak at the present time, because of the large uncertainties in the observations, it might become a more solid point as more reliable measurements of the chemical composition and cosmic ray spectrum in this energy region become available. It is crucial that future experiments give priority to the measurement of the chemical composition in the energy region between 10^{17} eV and 10^{19} eV.

The relatively steep injection spectrum required by the TWA scenario may be

problematic in that it appears to contradict the common wisdom that strong shock waves accelerate particles to flat spectra (typically E^{-2}). However, as discussed in Sec. 2, this is a rather oversimplified conclusion as both non-relativistic shocks and relativistic shocks can accelerate particles with steeper (as well as flatter) spectra in realistic situations: for instance a shock wave with Mach number 2.6 generates a power law with slope 2.7, although the acceleration efficiency is probably rather low, due to the low value of the Mach number. For relativistic shocks, the spectrum of accelerated particles, as discussed in Sec. 2, may depend on the equation of state. In Sec. 2.2 we showed an instance in which a shock with speed $u = 0.9$ generates accelerated particles with slope 2.7. Clearly none of these situations is universal, but these cases serve the scope of pointing out that this alleged discrepancy between the slope required by the TWA model and the expectation from the theory of shock acceleration cannot be taken too seriously. Moreover, both luminosity evolution of the sources (dashed line in Fig. 6), and the overlap of the contribution from numerous sources with different maximum energies at the source⁷¹ can produce a dip in the diffuse cosmic ray spectrum and at the same time may require relatively flat injection spectra.

A more serious concern for the TWA model is related to the chemical composition: the dip is in fact likely to disappear if a small contamination (with solar-like abundance) of nuclei heavier than hydrogen is present at the source^{65,72}. In this respect Helium appears to be the most *dangerous* in terms of affecting the conclusions of the model. Magnetic horizon effects related with nuclei with different charge to mass ratio might somewhat mitigate the relevance of this issue⁷³.

4. Spectrum and small scale anisotropies of UHECRs

A solid prediction of particle physics is that the photopion reactions of protons on the cosmic microwave background during their journey from the sources to Earth in the intergalactic space should induce a suppression in the diffuse spectrum of cosmic rays. This suppression, usually referred to as the GZK feature¹, appears at energy $\sim 10^{20}$ eV as a consequence of the relatively short interaction length, large inelasticity of the reaction of photopion production and due to the fact that the reaction has a kinematic threshold at roughly this energy (in fact the reaction starts taking place for lower energy protons when they scatter against the CMB photons on the tail of the Planck distribution, but most interactions occur with the photons on the peak). In Fig. 7 we show the loss length as a function of the energy of protons. We see that: *a)* the loss length at 10^{20} eV (slightly above threshold for $p + \gamma \rightarrow \pi + \text{anything}$) is ~ 100 Mpc while at energies two times smaller (slightly below threshold) it is almost as large as the size of the universe (horizontal line). The corresponding flux of cosmic rays at these energies is expected to drop roughly by the ratio of the loss lengths if the sources have a spatially homogeneous distribution. The exact amount of the suppression is however quite sensitive to the injection spectrum, to the maximum energy at the source, to the redshift evolution

of the sources and to the spatial distribution of the sources; *b*) at energy $\sim 2 \times 10^{18}$ eV the loss length, dominated by the process of proton pair production, equals the loss length due to the expansion of the universe (adiabatic losses).

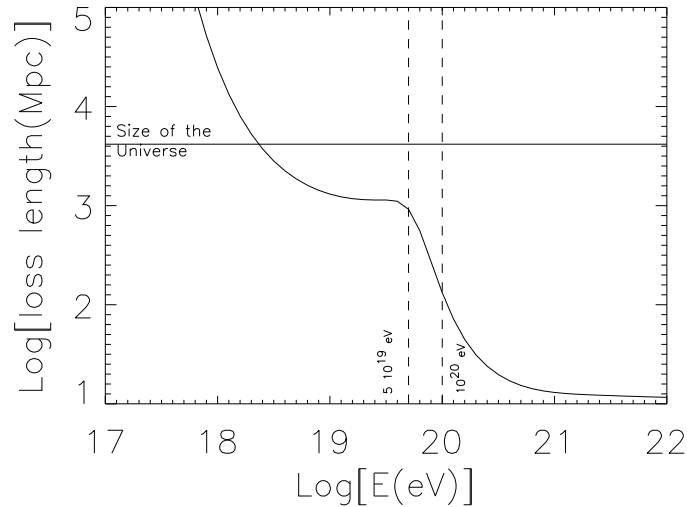


Fig. 7. Combined loss length for Bethe-Heitler pair production and photopion production on the photons of the cosmic microwave background. The horizontal dashed line shows the size of the universe and therefore the onset of adiabatic energy losses.

While the first point (point *a*) gives rise to the GZK feature, the second (point *b*) determines the appearance of the dip, discussed in Sec. 3^{64,65}.

The very low number of events expected at energies around and above 10^{20} eV makes the detection of the GZK feature very problematic. Experiments that have operated so far have not been successful in either detecting the GZK feature or proving its absence with a sufficiently high statistical significance. The spectra of AGASA, HiRes and the newly released data from the Pierre Auger telescope⁷⁶ are plotted in Fig. 8.

In⁷⁷ a careful Monte Carlo simulation of the propagation of cosmic rays from homogeneously distributed sources allowed the authors to infer the statistical significance of the AGASA and HiRes data available at the time. Neither one of the two experiments was found to have reached a definitive conclusion on the presence or absence of the GZK feature. AGASA and HiRes have a systematic offset in the absolute flux normalization that can however be understood if a relative systematic error in the energy determination of $\sim 30\%$ is assumed.

The results of⁷⁷ were recently confirmed and discussed in more detail in⁷⁸.

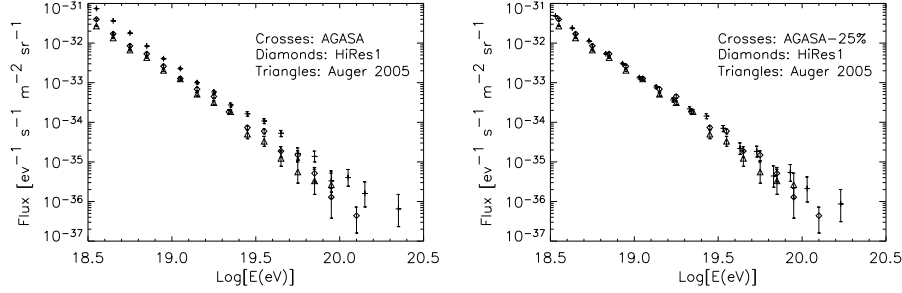


Fig. 8. *Left Panel*) Spectrum of AGASA, HiRes and Auger. *Right Panel*) Spectrum of AGASA, HiRes and Auger with a correction of the AGASA energy for a possible systematic error in the energy determination by -25% .

The authors simulated the AGASA spectrum normalizing at 4×10^{19} eV with a 30% statistical error in the energy determination of the events. The simulations were ran for 30000 realizations of spectra with 72 events above 4×10^{19} eV like in the AGASA data and the number of events with energies above 10^{20} eV in each realization were recorded. Taking into account the crucial non-gaussian distribution of the simulated data, the simulations show that the probability of having 11 or more events (as in AGASA) is 6×10^{-4} . In terms of gaussian probabilities this would correspond to about 3.2σ . The role of systematic errors was also investigated in ⁷⁸: the authors conclude that the AGASA data are compatible with the presence of a GZK feature at the 2.5σ level (in terms of gaussian errors). A similar exercise carried out on the HiRes data also results in the conclusion that HiRes data are *away* from AGASA data only at the 2σ level ⁷⁸.

These statistical considerations are the result of averages over large samples of realizations of source distributions, therefore one might wonder whether the individual spectra of those realizations which have a large number of events at ultra high energies are similar to the AGASA spectrum or not. In Fig. 9 we plot the spectra of some of the realizations that showed 11 or more events above 10^{20} eV (the error bars here are just poissonian, namely they have the same meaning as in Fig. 8). These spectra closely resemble the AGASA spectrum and all of them show no evidence of a GZK suppression, despite the fact that in the lower energy region they all fit the data quite well. This shows that an AGASA-like spectrum is not that improbable, even if the *average* cosmic ray spectrum can be expected to show a GZK feature ⁷⁸.

The spectrum of cosmic rays by itself does not contain enough information to determine the type of sources of UHECRs. A first hint at the type of sources can come from the identification of small clusters of events with arrival directions within the error box of the experiment. Such a signal of small scale anisotropies (SSA) was first claimed by the AGASA collaboration ⁷⁹. The signal was however shown to

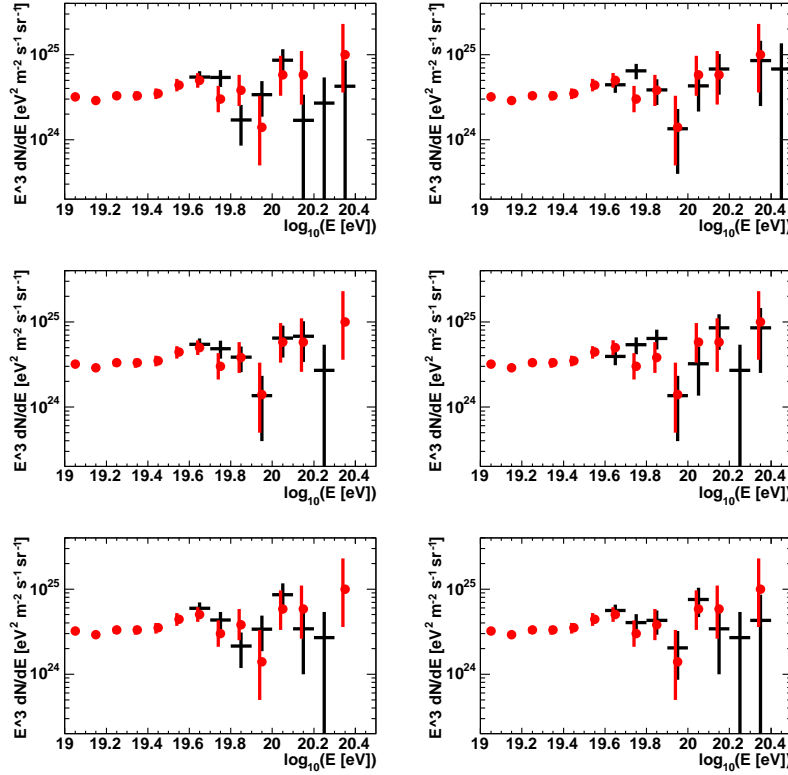


Fig. 9. Some of the simulated realizations with number of events equal to or larger than the actual number detected by AGASA ⁷⁸.

have a low statistical significance ⁸⁰. On the other hand, if astrophysical point sources are believed to accelerate UHECRs and if the intergalactic magnetic field is sufficiently low, then SSA are to be expected. It was shown in Ref. ⁸¹ that, if the AGASA results were confirmed, the number density of sources could be estimated to be around 10^{-5}Mpc^{-3} , with a quite large uncertainty due to the very limited statistics of events available (see ⁸² for other estimates). In ⁷⁸ the authors show that the spectrum of AGASA appears to be not fully consistent with the detection of the SSA by the same experiment. The possibility of coupling the information on the spectrum and SSA to gather better information on the number of sources will probably prove useful with the upcoming data from the Pierre Auger Collaboration.

The role of intergalactic magnetic fields in changing the spectrum and clustering of UHECRs is badly constrained as different simulations give different estimates for the magnitude and spatial structure of these fields (see, e.g., ^{83,84,85,86}). A homogeneous magnetic field spread through the whole Universe would leave the spectrum of diffuse cosmic rays unchanged with respect to the case of the absence

of magnetic field⁸⁷. The intergalactic magnetic fields can be neglected for particles with energies above 4×10^{19} eV if the magnetic field in the intergalactic medium is less than ~ 0.1 nG (reversal scale of 1 Mpc) and the small scale anisotropies are evaluated on angles of ~ 2 degrees⁸¹. This field magnitude is compatible with observational bounds⁸⁸ and detailed numerical simulations^{83,84} (however, see^{85,86} for different results). In these numerical simulations the magnetic field is assumed to be formed at some early time (seed field) and later amplified during the formation of the large scale structure of the Universe. The initial seed field can be due to some battery mechanism at shock fronts formed at the turn-around surfaces of large scale structures or may be of primordial origin⁸⁹. It might also have been spread into the universe during the early stages of evolution of galaxies⁹⁰. In many of these cases however the resulting magnetic fields are rather model dependent and are affected by further evolution of magnetic fields in the surrounding medium. In particular, the evolution due to the formation of large scale structures as found in simulations affects all these scenarios. An upper limit on the initial seed field could be imposed by requiring that the cosmological evolution of the fields does not lead to exceed the strength of the magnetic field seen in some clusters of galaxies (a few μG).

As pointed out above, the statistical significance of the SSA found by AGASA is rather low, and quite larger statistics of events are needed in order to detect the small angle clustering, if present. These measurements need to be carried out at extremely high energies in order to avoid appreciable deflections by the galactic magnetic fields. No evidence of SSA has been found so far in the HiRes data⁹¹.

The search for the GZK feature in the spectrum of UHECRs has been for a long time the prominent goal of researchers in this field. One should however not forget that there is an independent challenge, which is that of identifying sources that can potentially host an accelerator able to energize particles to energies as high as $\sim 10^{20}$ eV or larger⁹². From the theoretical point of view, the most important development in the field of particle acceleration has been the possibility of strong magnetic field amplification at shocks, as discussed in Sec. 2. This mechanism however has currently received much attention only in connection to SNRs, where the highest energies that can be reached are much lower than $\sim 10^{20}$ eV.

From the observational point of view, the most problematic issue to explain is the lack of any counterparts to the Fly's eye event⁹³, with energy 3×10^{20} eV. The distance of the potential sources should be limited to roughly the loss length of protons with this energy (even less in the case of gamma rays), namely, from Fig. 7, ~ 20 Mpc. On such short distances the effect of magnetic fields in deflecting the particles from their direction, if any, should be negligible, and a clear identification of the source should therefore be possible. No candidate was instead found⁹⁴. This problem is still unsolved, though several possibilities have been discussed. Among these the most likely is probably that the source was *bursting*. The term *burst* here is used to indicate a phenomenon with duration shorter than the typical time delays

induced by magnetic fields either in the intergalactic medium or in the Galaxy itself.

5. Summary and Discussion

Understanding the origin of cosmic rays means providing an explanation for the acceleration and the propagation of these particles, for their chemical composition and for the way they generate secondary radiations that we end up observing either as sources or as diffuse radiation in the Galaxy (or may be in the intergalactic medium).

In the last few years we have moved significantly ahead in terms of achieving these goals: the KASCADE data strongly suggest that the all-particle spectrum is the result of different chemical components with rigidity dependent maximum energies. Each chemical component appears to have a pronounced knee where the slope of the observed spectrum changes rather drastically (opposite to the change of slope in the all-particle spectrum, which is instead rather small). It remains to be understood whether these knees are the result of propagation in the Galaxy or of the acceleration process. The KASCADE rigidity dependent knees suggest that the galactic cosmic rays should *end* at energies $\sim 10^{18}$ eV with a presumably Iron dominated chemical composition. This energy is quite smaller than the position of the ankle, so that the confirmation of this result would imply that the transition from a galactic to an extragalactic origin of cosmic rays should take place below the ankle. This would rule in favor of the alternative view that the region of the ankle, made of a second knee and a dip is the result of Bethe-Heitler pair production on extragalactic cosmic rays^{64,65}, although at the present time we are far from having proved the model right. In order to clarify this problem it is crucial that the chemical composition of cosmic rays between 10^{17} eV and 10^{19} eV is reliably measured. If the extragalactic cosmic ray spectrum is appreciably contaminated by heavier elements the TWA model of the transition also has problems^{72,65}.

From the theoretical point of view, after the proposal of^{44,45,46}, it seems that the acceleration of cosmic rays at the shock fronts of SNRs, together with the high acceleration efficiency of such shocks, may make the acceleration of protons (iron nuclei) up to a few 10^{16} eV (10^{18} eV) viable. It remains to be understood why we do not observe enough SNRs in the TeV range (see³ and references therein for an accurate discussion of this point).

Moving toward higher energies, the spectrum of cosmic rays with energy between 3×10^{18} eV and 5×10^{19} eV as measured by AGASA (and Akeno), HiRes and now Auger (listing only the experiments with comparable exposures at the present time), seems to be rather well determined. There is an offset in the absolute normalizations of the three experiments which however could be resolved by admitting a systematic error in the error determination (roughly 30%) by one or all of the three experiments, possibly reflecting different observational techniques. Unfortunately this small difference implies different conclusions as far as the detection of the GZK feature is concerned. This is the clear symptom of an insufficient statistics

of events, as shown quantitatively in 77,78.

A signal associated with small angle clustering of the arrival directions, initially claimed by the AGASA collaboration 79 also appears to be statistically shaky 80. Both these points should strongly drive the community to achieve the larger statistics of events necessary for a reliable measurement of the spectrum and for a careful identification of anisotropies, two preliminary steps to have a clue to the sources of ultra high energy cosmic rays. This drive is leading us to the Auger Telescope and will hopefully lead us to the detection of UHECRs from space, with EUSO-like 95 or OWL-like experiments 96.

Acknowledgments

The author is very grateful to R. Aloisio, E. Amato, V. Berezinsky, D. De Marco, D. Ellison and S. Gabici for constructive comments on the manuscript and ongoing collaboration. The authors also wishes to acknowledge the help of T. Stanev and J. Hörandel for providing different versions of Fig. 1. Finally, the author is grateful for the kind hospitality of KIPAC at SLAC and at Stanford University in october-november 2005.

References

1. K. Greisen, *Phys. Rev. Lett.* **16**, 748 (1966); G.T. Zatsepin and V.A. Kuzmin, *Sov. Phys. JETP Lett.* **4**, 78 (1966).
2. V.L. Ginzburg and S.I. Syrovatskii, *The Origin of Cosmic Rays* ed. H.S.H. Massey (Oxford: Pergamon) (1964).
3. A.M. Hillas, *J. Phys. G: Nucl. Part. Phys.* **31**, R95 (2005).
4. V.S. Berezinsky et al., *Astrophysics of Cosmic Rays* (Amsterdam: North Holland) (1990).
5. E. Fermi, *Phys. Rev.* **75**, 1169 (1949); E. Fermi, *Astrophys. J.*, **119**, 1 (1954).
6. G.F. Krymskii, *Soviet Physics - Doklady* **327**, 328 (1977).
7. R.D. Blandford and J.R. Ostriker, *Astrophys. J.* **221**, 29 (1978).
8. A.R. Bell, *MNRAS* **182**, 443 (1978).
9. R. Blandford and D. Eichler, *Phys. Rep.* **154**, 1 (1987).
10. L.O'C. Drury, *Rep. Prog. Phys.* **46**, 973 (1983).
11. E.S. Seo and V.S. Ptuskin, *Astrophys. J.* **431**, 705 (1994)
12. R. Ramaty, R.E. Lingenfelter and B. Kozlovsky, *Space Sc. Rev.* **99**, 51 (2001).
13. R. Schlickeiser, *Cosmic Ray Astrophysics*, Springer (2002).
14. P.O. Lagage and C.J. Cesarsky, *A&A* **118**, 223 (1983).
15. P.O. Lagage and C.J. Cesarsky, *A&A* **125**, 249 (1983).
16. J.F. McKenzie and H.J. Völk, *A&A* **116**, 191 (1982); *erratum*, *A&A* **136**, 378 (1984).
17. V.S. Ptuskin and V.N. Zirakashvili, *A&A* **403**, 1 (2003).
18. H.J. Völk and P.L. Piermann, *Astrophys. J. Lett.* **333**, L65 (1988).
19. P.L. Biermann, *A&A* **271** 649 (1993).
20. J.R. Hörandel, *A review of experimental results at the knee*, in the "Workshop on Physics of the End of the Galactic Cosmic Ray Spectrum", Aspen, April 25 - 29, 2005 (preprint astro-ph/0508014).
21. J.R. Hörandel, *Astropart. Phys.* **19**, 193 (2003).

22. T. Antoni, et al. (KASCADE Collab.), *Astropart. Phys.* **24**, 1 (2005).
23. L.O'C Drury, E. van der Swaluw, O. Carroll, preprint astro-ph/0309820.
24. L.O'C Drury and H.J. Völk, *Proc. IAU Symp.* **94**, 363 (1980).
25. L.O'C Drury and H.J. Völk, *Astrophys. J.* **248**, 344 (1981).
26. M.A. Malkov, *Astrophys. J.* **485**, 638 (1997).
27. M.A. Malkov, P.H. Diamond P.H. and H.J. Völk, *Astrophys. J. Lett.* **533**, 171 (2000).
28. P. Blasi, *Astropart. Phys.* **16**, 429 (2002).
29. P. Blasi, *Astropart. Phys.* **21**, 45 (2004).
30. P. Blasi, S. Gabici and G. Vannoni, *MNRAS* **361**, 907 (2005).
31. F.C. Jones and D.C. Ellison, *Space Sci. Rev.* **58**, 259 (1991).
32. A.R. Bell, *MNRAS* **225**, 615 (1987).
33. D.C. Ellison, E. Möbius and G. Paschmann, *Astrophys. J.* **352**, 376 (1990).
34. D.C. Ellison, M.G. Baring F.C. and Jones, *Astrophys. J.* **453**, 873 (1995).
35. D.C. Ellison, M.G. Baring F.C. and Jones, *Astrophys. J.* **473**, 1029 (1996).
36. H. Kang and T.W. Jones, *Astrophys. J.* **476**, 875 (1997).
37. H. Kang and T.W. Jones, *Astrophys. J.* **620**, 44 (2005).
38. H. Kang, T.W. Jones and U.D.J. Gieseler, *Astrophys. J.* **579**, 337 (2002).
39. M.A. Malkov and L.O'C Drury, *Rep. Prog. Phys.* **64**, 429 (2001).
40. E. Amato and P. Blasi, *A general solution to non-linear particle acceleration at non-relativistic shock waves*, *MNRAS Lett.*, in press (preprint astro-ph/0509673).
41. H.J. Völk and J.F. McKenzie, *Proc. 17th International Cosmic Ray Conference* (Paris) **9**, 246 (1981); H.J. Völk, L.O'C. Drury and J.F. McKenzie, *A&A* **130**, 19 (1984).
42. L.O'C. Drury and A.E.G. Falle, *MNRAS* **223**, 353 (1986).
43. D.C. Ellison, A. Decourchelle and J. Ballet, *A&A* **413**, 189 (2004).
44. S.G. Lucek and A.R. Bell, *MNRAS* **314**, 65 (2000).
45. A.R. Bell and S.G. Lucek, *MNRAS* **321**, 433 (2001).
46. A.R. Bell, *MNRAS* **353**, 550 (2004).
47. M.A. Malkov and P.H. Diamond, preprint astro-ph/0509235.
48. F. Aharonian, et al. (HESS Collab.), *Nature* **432**, 75 (2004) F. Aharonian, et al. (HESS Collab.), *A&A Lett.* **437**, 7 (2005);
49. M.G. Baring, D.C. Ellison, S.P. Reynolds, I.A. Grenier and P. Goret, *Astrophys. J.* **513**, 311 (1999).
50. H.J. Völk, E.G. Berezhko and L.T. Ksenofontov, *A&A* **433**, 229 (2005)
51. M. Pohl, H. Yan and A. Lazarian, *Astrophys. J. Lett.* **626**, 101 (2005).
52. M. Ostrowski and J. Bednarz, *A&A* **394**, 1141 (2002).
53. A. Achterberg, Y.A. Gallant, J.G. Kirk, A.W. Guthmann, *MNRAS*, 328, 393 (2001).
54. M. Lemoine and G. Pelletier, *Astrophys. J. Lett.* **589**, 73 (2003).
55. J.G. Kirk, A.W. Guthmann, Y.A. Gallant and A. Achterberg, *Astrophys. J.* **542**, 235 (2000).
56. J.G. Kirk, and P. Schneider, *Astrophys. J.* **315**, 425 (1987).
57. J.G. Kirk, and P. Schneider, *Astrophys. J.* **322**, 256 (1987).
58. M. Vietri, *Astrophys. J.* **591**, 954 (2003).
59. P. Blasi and M. Vietri, *Astrophys. J.* **626**, 877 (2005).
60. J.L. Synge, *The Relativistic Gas* (Amsterdam: North Holland) (1957).
61. D.C. Ellison, F.C. Jones and S.P. Reynolds, *Astrophys. J.* **360**, 702 (1990).
62. M.G. Baring and J.G. Kirk, *A&A* **241**, 329 (1991).
63. D.C. Ellison and G.P. Double, *Astropart. Phys.* **18**, 213 (2002).
64. V.S. Berezinsky, A. Gazizov and S. Grigorieva, Preprint hep-ph/0204357; V.S. Berezinsky, A. Gazizov and S. Grigorieva, Preprint astro-ph/0302483.
65. V.S. Berezinsky, A. Gazizov and S. Grigorieva, *Phys. Lett.*, **B612**, 147 (2005).

66. V.S. Berezinsky and S. Grigorieva, *Astron. Astroph.* **199**, 1 (1988).
67. M. Lemoine, *Phys. Rev.* **D71**, 3007 (2005).
68. R. Aloisio and V.S. Berezinsky, *Astrophys. J.* **625**, 249 (2005).
69. P. Blasi, R. Epstein and A.V. Olinto, *Astrophys. J. Lett.* **533**, 123 (2000).
70. J. Arons, *Astrophys. J.* **589**, 871 (2003).
71. M. Kachelriess and D. Semikoz, preprint astro-ph/0510188
72. D. Allard, E. Parizot, A.V. Olinto, E. Khan, S. Goriely, preprint astro-ph/0508465.
73. G. Sigl and E. Armengaud, preprint astro-ph/0507656.
74. M. Takeda et al. (AGASA Collaboration) *Astropart. Phys.* **19** 447 (2003).
75. T. Abu-Zayyad et al. (High Resolution Fly's Eye Collaboration) *Astropart. Phys.* **23** 157 (2005).
76. P. Sommers et al. (Auger Collaboration), *Proceedings of the 29th International Cosmic Ray Conference*, Pune, India (2005).
77. D. De Marco, P. Blasi and A.V. Olinto *Astropart. Phys.* **20** 53 (2003).
78. D. De Marco, P. Blasi and A.V. Olinto, preprint astro-ph/0507324.
79. M. Takeda et al. *Astrophys. J.* **522**, 225 (1999); Y. Uchihori et al. *Astropart. Phys.* **13**, 151 (2000); N. Hayashida et al. Preprint astro-ph/0008102.
80. C.B. Finley and S. Westerhoff, *Astropart. Phys.* **21**, 359 (2004).
81. P. Blasi and D. De Marco, *Astropart. Phys.* **20**, 559 (2004).
82. H. Yoshiguchi, S. Nagataki, S. Tsubaki and K. Sato, *Astrophys. J.* **586**, 1211 (2003); H. Yoshiguchi, S. Nagataki and K. Sato, *Astrophys. J.* **592**, 311 (2003); H. Takami, H. Yoshiguchi and K. Sato, Preprint astro-ph/0506203; S.L. Dubovsky, P.G. Tinyakov and I.I. Tkachev, *Phys. Rev. Lett.* **85**, 1154 (2000); Z. Fodor and S.D. Katz, *Phys. Rev.* **D63**, 023002 (2001).
83. K. Dolag, D. Grasso, V. Springel and I. Tkachev, *JETP Letters* **79**, 583 (2004); *Pisma Zh. Eksp. Teor. Fiz.* **79**, (2004).
84. K. Dolag, D. Grasso, V. Springel and I. Tkachev, *JCAP* **01**, 9 (2005).
85. G. Sigl, F. Miniati and T.A. Ensslin, *Phys. Rev.* **D68**, 3002 (2003).
86. G. Sigl, F. Miniati and T.A. Ensslin, *Phys. Rev.* **D70**, 3007 (2004).
87. R. Aloisio and V.S. Berezinsky, *Astrophys. J.* **612**, 900 (2004).
88. P. Blasi, S. Burles and A.V. Olinto, *Astrophys. J. Lett.* **514**, L79 (1999).
89. D. Grasso and H.R. Rubinstein, *Phys. Rep.* **348**, 163 (2001).
90. P.P. Kronberg, H. Lesch and U. Hopp, *Astrophys. J.* **511**, 56 (1999).
91. R.U. Abbasi et al. (HiRes Collaboration), *Astrophys. J. Lett.* **610**, 73 (2004).
92. A.V. Olinto, *Physics Reports* **333**, 329 (2000).
93. D.J. Bird et al. (Fly's Eye Collaboration), *Astrophys. J.* **441**, 144 (1995).
94. J.W. Elbert and P. Sommers, *Astrophys. J.* **441**, 151 (1995).
95. EUSO Collaboration, www.euso-mission.org.
96. OWL Collaboration, <http://owl.gsfc.nasa.gov>.